CLNS 04/1871
CLEO 04-5

First Observation and Dalitz Analysis of the $D^0 \to K^0_S\eta\pi^0$ Decay

P. Rubin,[1] C. Cawlfield,[2] B. I. Eisenstein,[2] G. D. Gollin,[2] I. Karliner,[2] N. Lowrey,[2] P. Naik,[2] C. Sedlack,[2] M. Selen,[2] J. J. Thaler,[2] J. Williams,[2] K. W. Edwards,[3] D. Besson,[4] K. Y. Gao,[5] D. T. Gong,[5] Y. Kubota,[5] S. Z. Li,[5] R. Poling,[5] A. W. Scott,[5] A. Smith,[5] C. J. Stepaniak,[5] J. Urheim,[5] Z. Metreveli,[6] K. K. Seth,[6] A. Tomaradze,[6] P. Zweber,[6] J. Ernst,[7] K. Arms,[8] E. Eckhart,[8] K. K. Gan,[8] H. Severini,[9] P. Skubic,[9] D. M. Asner,[10] S. A. Dytman,[10] S. Mehrabyan,[10] J. A. Mueller,[10] V. Savinov,[10] Z. Li,[11] A. Lopez,[11] H. Mendez,[11] J. Ramirez,[11] G. S. Huang,[12] D. H. Miller,[12] V. Pavlunin,[12] B. Sanghi,[12] E. I. Shibata,[12] I. P. J. Shipsey,[12] G. S. Adams,[13] M. Chasse,[13] J. P. Cummings,[13] I. Danko,[13] J. Napolitano,[13] D. Cronin-Hennessy,[14] C. S. Park,[14] W. Park,[14] J. B. Thayer,[14] E. H. Thorndike,[14] T. E. Coan,[15] Y. S. Gao,[15] F. Liu,[15] R. Stroynowski,[15] M. Artuso,[16] C. Boulahouache,[16] S. Blusk,[16] J. Butt,[16] E. Dambasuren,[16] O. Dorjkhaidav,[16] N. Menaa,[16] R. Mountain,[16] H. Muramatsu,[16] R. Nandakumar,[16] R. Redjimi,[16] R. Sia,[16] T. Skwarnicki,[16] S. Stone,[16] J.C. Wang,[16] K. Zhang,[16] A. H. Mahmood,[17] S. E. Csorna,[18] G. Bonvicini,[19] D. Cinabro,[19] M. Dubrovin,[19] A. Bornheim,[20] E. Lipeles,[20] S. P. Pappas,[20] A. J. Weinstein,[20] R. A. Briere,[21] G. P. Chen,[21] T. Ferguson,[21] G. Tatishvili,[21] H. Vogel,[21] M. E. Watkins,[21] N. E. Adam,[22] J. P. Alexander,[22] K. Berkelman,[22] D. G. Cassel,[22] J. E. Duboscq,[22] K. M. Ecklund,[22] R. Ehrlich,[22] L. Fields,[22] R. S. Galik,[22] L. Gibbons,[22] B. Gittelman,[22] R. Gray,[22] S. W. Gray,[22] D. L. Hartill,[22] B. K. Heltsley,[22] D. Hertz,[22] L. Hsu,[22] C. D. Jones,[22] J. Kandaswamy,[22] D. L. Kreinick,[22] V. E. Kuznetsov,[22] H. Mahlke-Krüger,[22] T. O. Meyer,[22] P. U. E. Onyisi,[22] J. R. Patterson,[22] T. K. Pedlar,[22] D. Peterson,[22] J. Pivarski,[22] D. Riley,[22] J. L. Rosner,[22,*] A. Ryd,[22] A. J. Sadoff,[22] H. Schwarthoff,[22] M. R. Shepherd,[22] W. M. Sun,[22] J. G. Thayer,[22] D. Urner,[22] T. Wilksen,[22] M. Weinberger,[22] S. B. Athar,[23] P. Avery,[23] L. Breva-Newell,[23] R. Patel,[23] V. Potlia,[23] H. Stoeck,[23] and J. Yelton[23]

(CLEO Collaboration)

[1] *George Mason University, Fairfax, Virginia 22030*
[2] *University of Illinois, Urbana-Champaign, Illinois 61801*
[3] *Carleton University, Ottawa, Ontario, Canada K1S 5B6 and the Institute of Particle Physics, Canada*
[4] *University of Kansas, Lawrence, Kansas 66045*
[5] *University of Minnesota, Minneapolis, Minnesota 55455*
[6] *Northwestern University, Evanston, Illinois 60208*
[7] *State University of New York at Albany, Albany, New York 12222*
[8] *Ohio State University, Columbus, Ohio 43210*
[9] *University of Oklahoma, Norman, Oklahoma 73019*
[10] *University of Pittsburgh, Pittsburgh, Pennsylvania 15260*
[11] *University of Puerto Rico, Mayaguez, Puerto Rico 00681*
[12] *Purdue University, West Lafayette, Indiana 47907*
[13] *Rensselaer Polytechnic Institute, Troy, New York 12180*
[14] *University of Rochester, Rochester, New York 14627*
[15] *Southern Methodist University, Dallas, Texas 75275*
[16] *Syracuse University, Syracuse, New York 13244*
[17] *University of Texas - Pan American, Edinburg, Texas 78539*

[18] *Vanderbilt University, Nashville, Tennessee 37235*
[19] *Wayne State University, Detroit, Michigan 48202*
[20] *California Institute of Technology, Pasadena, California 91125*
[21] *Carnegie Mellon University, Pittsburgh, Pennsylvania 15213*
[22] *Cornell University, Ithaca, New York 14853*
[23] *University of Florida, Gainesville, Florida 32611*
(Dated: September 7, 2004)

Abstract

Using 9.0 fb^{-1} of integrated luminosity in e^+e^- collisions near the Υ(4S) mass collected with the CLEO II.V detector we report the first observation of the decay $D^0 \to K^0_S\eta\pi^0$. We measure the ratio of branching fractions, $\frac{BR(D^0\to K^0_S\eta\pi^0)}{BR(D^0\to K^0_S\pi^0)} = 0.46 \pm 0.07 \pm 0.06$. We perform a Dalitz analysis of 155 selected $D^0 \to K^0_S\eta\pi^0$ candidates and find leading contributions from $a_0(980)K^0_S$ and $K^*(892)\eta$ intermediate states.

*On leave of absence from University of Chicago.

A large fraction of the known D meson decay rate is in three-body hadronic decays to the pseudoscalar particles K and π. These decays dominantly proceed through quasi-two-body intermediate states with a rich set of resonances. The dynamics of three body decays can be studied using the Dalitz technique [1]. Interest in the decay $D^0 \to K^0_S\eta\pi^0$ stems from comparing the results of the Dalitz plot analyses of the decay $D^0 \to K^0_S\pi^+\pi^-$ studied by ARGUS[2] and CLEO[3] with the decay $D^0 \to K^0_S K^+K^-$ studied by ARGUS[4] and BaBar[5]. The contribution of the $f_0(980)$ observed in the former case is not enough to explain the $\sim$60% fraction observed in the latter decay. Additional scalar contribution from $a_0(980)K^0_S$ can be expected in $D^0 \to K^0_S K^+K^-$, but is difficult to separate from $f_0(980)K^0_S$ in the Dalitz plot. The $a_0(980)K^0_S$ intermediate state can also be observed in the favored $a_0(980) \to \eta\pi^0$ decay mode which would give rise to the $D^0 \to K^0_S\eta\pi^0$ final state. The decay $D^0 \to K^0_S\eta\pi^0$ or any other D^0 modes with $a_0(980)$ in the intermediate state have not yet been observed. There is little information on D^0 decay modes with η in the final state; only an upper limit $BR(D^0 \to \eta X) < 13\%$ @ $C.L. = 90\%$ [6] has been measured. Note that $K^0_S\eta\pi^0$ is a CP eigenstate. A large sample with a good signal to noise ratio in this mode can be used for studies of CP violation in D^0 and $\overline{D^0}$ decays.

The data sample used in this analysis was produced by the Cornell Electron Storage Ring (CESR) and collected with the general purpose CLEO II.V [7] detector. Our analysis is based on 9.0 fb^{-1} of integrated luminosity of e^+e^- collisions at $\sqrt{s} \simeq 10$ GeV above and below $B\bar{B}$ production threshold. Charmed particles can be produced both in the process $e^+e^- \to c\bar{c}$ and in B meson decays. To suppress events with low momentum D^0's from B decays, which have higher multiplicity and higher combinatorial backgrounds, we use the decay $D^{*+} \to D^0\pi^+$ (charge conjugation is implied throughout this letter) as a tag and require that the D^{*+} momentum exceeds 2.8 GeV/c. The decay $D^0 \to K^0_S\eta\pi^0$ is observed in the most probable mode of the final state, $K^0_S \to \pi^+\pi^-$, $\eta \to \gamma\gamma$, $\pi^0 \to \gamma\gamma$.

Charged tracks are required to be well measured in the tracking detectors. Candidate K^0_S-s are reconstructed from pairs of oppositely charged tracks assumed to be pions. The candidate K^0_S trajectory is required to be consistent with production in the interaction region, while its vertex should be significantly ($> 10\sigma$) isolated from this region. We select K^0_S candidates if the reconstructed mass, $m_{\pi^+\pi^-}$, is within 10 MeV/c^2 of the nominal K^0_S mass [6]. On average, K^0_S-s in this selection have a mass resolution of $\sigma_{K^0_S} = 3.7\pm0.2$ MeV/c^2.

We form π^0 and η candidates from pairs of neutral showers in the CLEO CsI calorimeter. They are required to be consistent with electromagnetic showers, have an energy deposition above 30 MeV and be in the central, barrel region of the detector. For π^0 candidates we require the invariant mass, $m_{\gamma\gamma}$, of the photon pair to be within 18 MeV/c^2 of the nominal π^0 mass [6]. The average detector resolution of $\pi^0 \to \gamma\gamma$ invariant mass is $\sigma_{\pi^0} = 6.1 \pm 1.2$ MeV/c^2. Similarly, η candidates are required to have a two photon invariant mass within 40 MeV/c^2 of the nominal η mass [6] at the average detector resolution of $\sigma_\eta = 12.6 \pm 1.0$ MeV/c^2.

We kinematically fit K^0_S, π^0 and η candidates and constrain their masses to nominal values. This procedure improves the D^0 mass resolution by a factor of two for $D^0 \to K^0_S\eta\pi^0$ decays. We reconstruct $D^0 \to K^0_S\eta\pi^0$ candidates by combining the K^0_S, π^0 and η candidates in the event. To eliminate the significant combinatoric background, we select the combination with the smallest $\chi^2_m = \left(\frac{m_{\gamma\gamma}-m_\eta}{\sigma_\eta}\right)^2 + \left(\frac{m_{\gamma\gamma}-m_{\pi^0}}{\sigma_{\pi^0}}\right)^2 + \left(\frac{m_{\pi^+\pi^-}-m_{K^0_S}}{\sigma_{K^0_S}}\right)^2$, where all the invariant masses are taken

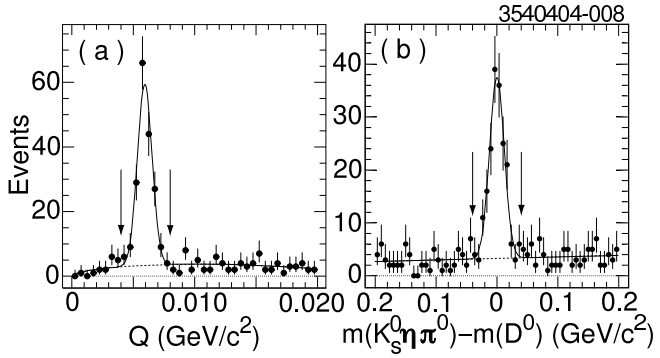

FIG. 1: Distribution of the energy release, Q, in the decay $D^{*+} \to D^0\pi^+$ (a), and the mass difference of $D^0 \to K^0_S\eta\pi^0$ candidates (b).

before the mass constraint of the kinematic fit.

The D^0 candidate is combined with π^+ tracks to form the tagging decay $D^{*+} \to D^0\pi^+$. A significant D^0 signal is observed both in the energy release, $Q = m(K^0_S\eta\pi^0\pi^+) - m(K^0_S\eta\pi^0) - m_{\pi^+}$, and in the D^0 mass difference $\Delta m = m(K^0_S\eta\pi^0) - m_{D^0}$ shown in Fig. 1. The Q distribution, shown in Fig. 1a, represents raw Q vs Δm events in $\sim 3\sigma$ signal Δm band indicated by arrows in Fig. 1b and vice versa.

We estimate a signal yield of 155±22 events from a fit with a single Gaussian for the signal plus a linear background to the mass spectrum of Fig. 1(b). The GEANT-based Monte Carlo simulation [8] of the CLEO II.V detector response is used to estimate the efficiency $\varepsilon(D^0 \to K^0_S\eta\pi^0) = (1.15 \pm 0.05 \pm 0.12 \pm 0.01)\%$, where the uncertainties are statistical, systematic and from the uncertainties on the $K^0_S \to \pi^+\pi^-$, $\eta \to \gamma\gamma$, $\pi^0 \to \gamma\gamma$ branching fractions, respectively. The systematic uncertainty includes the track reconstruction efficiency (2%/track), π^0 and η selection (5% each), and the background subtraction in D^0 mass spectrum (7.2%). The first two uncertainties absorb a variation of efficiency between the phase space and the resonant event production mechanism. The background subtraction error is estimated from variation in the signal yield when we change the fit function including a single versus double Gaussian for the signal and background described with a linear function, taken from the D^0 mass spectrum sidebands, or taken from the Q distribution sidebands.

To measure the branching fraction we normalize to the total number of D^0's produced in the decay $D^{*+} \to D^0\pi^+$. We use the $D^0 \to K^0_S\pi^0$ decay with known rate, $BR(D^0 \to K^0_S\pi^0) = \frac{1}{2}BR(D^0 \to \overline{K}^0\pi^0) = (1.14 \pm 0.11)\%$ [6]. We use the same selection as $D^0 \to K^0_S\eta\pi^0$, but without the η, and find a very clean $D^0 \to K^0_S\pi^0$ signal with yield of 1105±54 events and an efficiency $\varepsilon(D^0 \to K^0_S\pi^0) = (3.76 \pm 0.18 \pm 0.26 \pm 0.02)\%$. We find the ratio of branching fractions to be $\frac{BR(D^0 \to \overline{K}^0\eta\pi^0)}{BR(D^0 \to \overline{K}^0\pi^0)} = \frac{BR(D^0 \to K^0_S\eta\pi^0)}{BR(D^0 \to K^0_S\pi^0)} = 0.46 \pm 0.07 \pm 0.06 \pm 0.003 = 0.46 \pm 0.09$, where the errors are statistical, systematic, and $\eta \to \gamma\gamma$ branching fraction uncertainties, respectively. Using the known $D^0 \to K^0_S\pi^0$ branching fraction, we find $BR(D^0 \to \overline{K}^0\eta\pi^0) = (1.05 \pm 0.16 \pm 0.14 \pm 0.10)\%$, where the last error is associated with the uncertainty on the $D^0 \to K^0_S\pi^0$ branching fraction. Many systematic uncertainties cancel in the ratio measurement.

The selected sample, although small, is clean enough to search for possible intermediate states using the Dalitz technique [9]. We tighten the mass difference selection criteria to

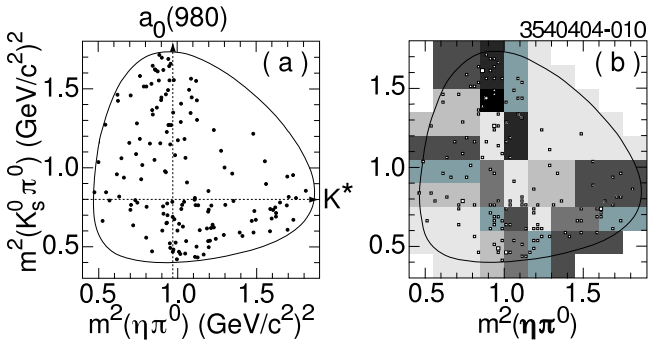

FIG. 2: Dalitz plot of $D^0 \to K^0_S\eta\pi^0$ (a), and the map for the adaptive binning (b).

two standard deviations ($|\Delta m| < 25$ MeV/c^2 and $|\Delta Q| < 1.2$ MeV/c^2) in order to increase signal to background ratio. We select for Dalitz analysis 155 events (accidentally the same number of events that we find for measurement of the branching ratio) shown in Fig. 2(a) as $m^2(\eta\pi^0)$ versus $m^2(K^0_S\pi^0)$. The same selection criteria were applied to measure the efficiency across the Dalitz plot with a simulation of $D^0 \to K^0_S\eta\pi^0$ decaying uniformly in its allowed phase space. The shape of the small background is taken from the data sample of 171 events in a Q sideband, $10 < Q < 25$ MeV/c^2, and an extended range of invariant mass, $|\Delta m| < 100$ MeV/c^2. Both the efficiency and the background are nearly uniform across the Dalitz plot and we parameterize them separately with a two-dimensional polynomial of third degree obtained from the dedicated fit.

The Dalitz plot, Fig. 2(a), shows a significant contribution from $a_0(980)K^0_S$ interfering with other resonances, as evidenced by the deficit of event density in the center of the plot, and by the shift to the left (right) of the $a_0(980)$ band on the top (bottom) of the plot. There is an indication of a $K^*(892)\eta$ contribution as there is an enhancement in the expected region in the $m^2(K^0_S\pi^0)$ projection, shown in Fig. 3(a). The visible mass peak is shifted lower than would be expected given the $K^*(892)$ mass indicating interference of $K^*(892)\eta$ with other intermediate states.

To extract information from the Dalitz plot we apply the technique developed in our previous analyses [9], [3] which uses an unbinned maximum likelihood fit and an "isobar model" to measure matrix element amplitudes. An isobar model approximates the matrix elements as
$\mathcal{M} = a_{_{NR}} e^{i\varphi_{NR}} + \sum_{_R} a_R e^{i\varphi_R} \mathcal{A}_J(\{K^0_S, \eta, \pi^0\}|R)$,
a coherent sum of non-resonant (NR) and resonance (R) terms, each multiplied by its own complex factor. The complex factor is parametrized by a real amplitude $a_{_R}$ and a phase $\varphi_{_R}$, which are extracted from the fit. The amplitude, $\mathcal{A}_J(ABC|R)$, is defined for the decay chain $D^0 \to RC \to ABC$ with an intermediate resonance R represented by the Breit-Wigner function with spin J dependent factor. The overall amplitude normalization and complex phase are arbitrary, and are chosen such that $a_{a_0} = 1$, $\varphi_{a_0} = 0$.

The mass m dependent width of the $a_0(980)$ is parameterized using the method of Flatte [10], while the partial width is proportional to the phase space factor $\rho = 2p/m$ instead of the decay momentum p,
$m\Gamma_{a_0(980)}(m) = \frac{g^2_{a_0\eta\pi^0}}{16\pi}\rho_{\eta\pi^0} + \frac{g^2_{a_0K^+K^-}}{16\pi}\left(\rho_{K^+K^-} + \rho_{K^0\bar{K}^0}\right)$. We assume an isospin symmetry for the coupling constants, $g^2_{a_0\eta\pi^+} = g^2_{a_0\eta\pi^0}$ and $g^2_{a_0K^+K^-} = g^2_{a_0K^0\bar{K}^0} = g^2_{a_0K^0K^+}/2$. In our standard fit we use $a_0(980)$ parameters from [11], $m(a_0(980)) = 999 \pm 5$ MeV/c^2,

$g^2_{a_0\eta\pi^0} = 11.1 \pm 1.0$ GeV^2, $g^2_{a_0K^+K^-}/g^2_{a_0\eta\pi^0} = 0.58 \pm 0.09$.

The event density of the Dalitz plot is fit to the efficiency corrected matrix element squared and the background polynomial which is added incoherently [9] to the signal. The relative signal fraction, 0.867 ± 0.027, is estimated from the Δm spectrum of the data sample. In all Dalitz fits the signal fraction is a parameter of the fit constrained to this estimate.

With our sample we find the most reliable goodness of fit estimator to be a χ^2-like parameter for Poisson statistics: $\chi^2 = \sum_{i=1}^{N} \frac{(n_i-\nu_i)^2}{\nu_i}$, [6] where n_i, ν_i are the number of events and its mean expectation in the i-th bin, and N is a total number of bins. We split the Dalitz plot into 10×10 equal bins. In order to provide sufficient statistics for a mean expectation, it was necessary to join some bins using so-called "adaptive binning" and requiring ν_i (or n_i)>5 in each bin. The 24 bins found with adaptive binning are shown in Fig. 2(b). We have tested this goodness of fit parameter in simplified Monte-Carlo based simulations of our data and find that it gives a uniform probability for statistically distributed data with $P(\chi^2/N_{d.o.f.})$ in the range [0,1]. The simulation of different models shows that we are only sensitive to contributions to the Dalitz plot that are greater than 20% of the total rate, and thus our goal is to find a consistent description of the observed event density using a minimal set of dominant modes.

From previous observations [6] we expect $\eta\pi^0$ to have contributions from intermediate states including $a_0(980)$, $a_2(1320)$, and $a_0(1450)$. Similarly, $K^0_S\pi^0$ should have contributions from $K^*(892)$, $K^*_1(1410)$, $K^*_0(1430)$, $K^*_2(1430)$, and $K^*_1(1680)$. A possible low-mass $K\pi$-scalar state or dynamical structure, κ, which is not included in [6] but is widely discussed in recent publications [12], could also contribute. There is no obvious contribution from $K^0_S\eta$ in this mass range. We start with a minimal set of resonances and recognize an additional resonance as contributing if the fit probability improves, the amplitude is at least three standard deviations from zero, and the error on the phase is less than 30°.

We find that a model including only $a_0(980)K^0_S$ and $K^*(892)\eta$ contributions gives a low probability of 0.8% and is an unlikely explanation of our data. Models with a single resonance are even worse with probabilities of less than 10^{-6}. Good consistency with our data can be achieved with models including two main intermediate states, $a_0(980)K^0_S$, $K^*(892)\eta$, and additional mode(s). We find four additional modes giving a fit probability >1%: (i) a non-resonant fraction; (ii) $K^*_0(1430)\eta$; (iii) $K^*_0(1430)\eta$ and $a_2(1320)K^0_S$ (fit projections are shown in Fig. 3); and (iv) a κ with parameters taken from [12]. We do not find any significant contribution or fit quality improvement by adding other resonances. For these four models Table I summarizes the amplitude and phase we extract from the fit for the $K^*(892)\eta$ mode, fixing the amplitude and phase for the $a_0(980)K^0_S$ mode to be one and zero respectively. Our sample is too small to allow us to choose one model among these four. In the last row of Table I we present averaged results and their variation due to our inability to choose a single decay model that describes our data adequately.

When the amplitudes and phases are extracted from the fit we derive the fit fraction (FF) for each contribution. The fit fraction is defined for each resonance as its matrix element amplitude squared (rate) integrated over the allowed phase space divided by the total matrix element amplitude squared integrated over the same phase space. In general the sum of the fit fractions does not have to equal one due to interference among the contributions. A statistical uncertainty on the fit fraction is computed from the fit covariance matrix using Monte Carlo methods as described in [9]. Table I gives the fit fractions for the $a_0(980)K^0_S$ and $K^*(892)\eta$ modes, and the fit fraction for the additional mode(s), their averaged values, and estimated variations due to the choice of decay model.

TABLE I: Results for four models of the additional contribution beyond $a_0(980)K^0_S$ and $K^*(892)\eta$ to $D^0 \to K^0_S\eta\pi^0$. The amplitude and phase for $a_0(980)K^0_S$ are fixed to 1 and 0° respectively. The uncertainties are statistical from the fit. "FF(Add.)" means the sum of the fit fractions for all modes in addition to $a_0(980)K^0_S$ and $K^*(892)\eta$ in the model. The last row shows averaged values with statistical uncertainties and half the range among the four decay models.

Additional Mode(s)	$a_{K^*(892)\eta}$	$\varphi_{K^*(892)\eta}(^\circ)$	FF($a_0(980)K^0_S$)	FF($K^*(892)\eta$)	FF(Add.)
NR	.234±.035	260±10	1.350±0.097	.301±.071	.288±.113
$K^*_0(1430)\eta$	.237±.032	258±10	1.322±0.070	.301±.070	.360±.115
$K^*_0(1430)\eta + a_2(1320)K^0_S$	.253±.031	251±15	1.042±0.146	.273±.050	.316±.097
$\kappa\eta$	.269±.032	262±11	1.050±0.060	.310±.060	.186±.056
Average and {Variation}	.249±.032 {.018}	259±12 {6}	1.187±0.093 {0.154}	.293±.062 {.019}	.246±.092 {.087}

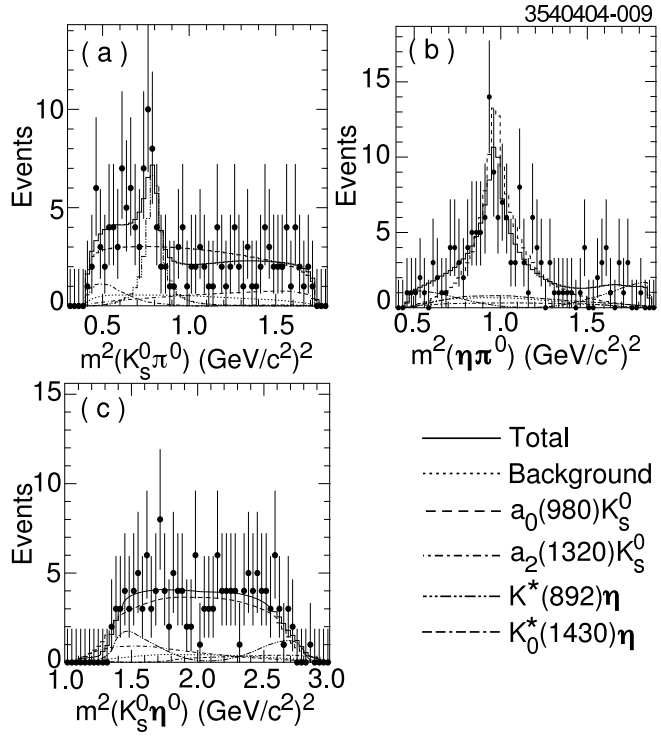

FIG. 3: The three projections of the Dalitz plot. The fit shown has contributions from $a_0(980)K^0_S$, $K^*(892)\eta$, $K^*_0(1430)\eta$, and $a_2(1320)K^0_S$.

We consider possible sources of systematic uncertainties due to the background, the efficiency, the finite detector resolution, the parameterization of the matrix element amplitude, and choice of decay model. Central values are taken as the statistical weighted mean of the results summarized in Table I.

For the background and the efficiency we perform the fit with the two-dimensional polynomial coefficients allowed to float constrained by their covariance matrices. We also hold the efficiency constant across the Dalitz plot. Deviations from the standard fit are treated

as systematic uncertainties. The effects are small.

As a consistency check, we allow the parameters of one of the clearly observed resonances to float and extract values from the fit. For both the $K^*(892)$ and $a_0(980)$ we obtain masses, and width parameters consistent with previously measured values.

Our mass resolution, small compared to the widths of the resonances we are considering, is a negligible effect as we observe no change when we do a fit that smears each resonance by a two dimensional Gaussian with widths given by propagating uncertainties on track fits and shower reconstructions.

We also consider variations in the description of the decay amplitudes. We vary the radial parameters for the intermediate resonances between zero and twice their standard value of ~ 3 GeV^{-1} [9]. We allow the masses and widths for the intermediate resonances to vary within one standard deviation of their measured values [6]. The largest variation from the standard fit of each fit parameter is taken as an uncertainty. These uncertainties are combined quadratically to give a systematic uncertainty.

The largest systematic uncertainty results from choice of decay model. Using the four models giving good fits we take half the range of central values, shown in Table I, as this uncertainty and report it separately.

Our analysis apparently contradicts a result done with an earlier version of our detector $BR(D^0 \to \overline{K}^*(892)\eta) = (1.8 \pm 0.4)\%$ [6, 13, 14]. That analysis, which focused on a search for this mode, made helicity angle and η momentum selections that are not compatible with a $K^0_S\eta\pi^0$ Dalitz analysis. Thus the effects of interference were not considered. Comparing the fit result to the $K\pi$ mass spectrum in [14] with results obtained in this analysis we find that the $D^0 \to \overline{K}^*(892)\eta$ rate is larger by roughly a factor of two.

In conclusion, we have observed for the first time the decay $D^0 \to K^0_S\eta\pi^0$. We have measured the ratio of the branching fractions,

$$\frac{BR(D^0 \to K^0_S\eta\pi^0)}{BR(D^0 \to K^0_S\pi^0)} = 0.46 \pm 0.07 \pm 0.06, \tag{1}$$

where the uncertainties are statistical and systematic respectively. Using the known $D^0 \to K^0_S\pi^0(\overline{K^0}\pi^0)$ decay rate we measure the branching fraction

$$BR(D^0 \to \overline{K}^0\eta\pi^0) = (1.05 \pm 0.16 \pm 0.14 \pm 0.10)\%, \tag{2}$$

where the final uncertainty is associated with the $D^0 \to \overline{K}^0\pi^0$ branching fraction.

We have analyzed the resonant substructure of the decay $D^0 \to K^0_S\eta\pi^0$ using the Dalitz technique. We find dominant contributions from $a_0(980)K^0_S$ and $K^*(892)\eta$ intermediate states. Using an isobar model including $K^*(892)\eta$, $a_0(980)K^0_S$, and averaging over four consistent models for additional components we find the amplitude, phase and fit fractions

$$\begin{gathered} a_{K^*(892)\eta} = 0.249 \pm 0.032 \pm 0.013 \pm 0.018, \\ \varphi_{K^*(892)\eta} = (259 \pm 12 \pm 9 \pm 6)^\circ, \\ FF(K^*(892)\eta) = 0.293 \pm 0.062 \pm 0.029 \pm 0.019, \\ FF(a_0(980)K^0_S) = 1.19 \pm 0.09 \pm 0.20 \pm 0.16, \end{gathered} \tag{3}$$

where $a_{a_0K^0_S}$ and $\varphi_{a_0K^0_S}$ are fixed to one and zero respectively. The uncertainties are statistical, systematic, and decay model choice respectively. We also find that contributions from $a_0(980)K^0_S$ and $K^*(892)\eta$ are not sufficient to describe our data. We estimate the fit fraction of any additional component as

$$FF(\text{Add.}) = 0.246 \pm 0.092 \pm 0.025 \pm 0.087, \tag{4}$$

with the uncertainties meaning as above.

We gratefully acknowledge the effort of the CESR staff in providing us with excellent luminosity and running conditions. This work was supported by the National Science Foundation and the U.S. Department of Energy.

---

[1] R. H. Dalitz, Phil. Mag. 44, 1068 (1953).
[2] H. Albrecht *et al.* (ARGUS Collaboration), Phys. Lett. **B308**, 435 (1993).
[3] H. Muramatsu *et al.* (CLEO Collaboration) , Phys. Rev. Lett. **89**, 251802 (2002) [Erratum-ibid. **90**, 059901 (2003).
[4] H. Albrecht *et al.* (ARGUS Collaboration), Z. Phys. C **33**, 359 (1987).
[5] B. Aubert *et al.* (BABAR Collaboration), SLAC-PUB-9320, in Proceedings of ICHEP 2002, 31st, Amsterdam, The Netherlands, 24-31 Jul 2002.
[6] Particle Data Group, Review of Particle Physics, Phys. Rev. D **66**, 010001 (2002).
[7] Y. Kubota *et al.*, Nucl. Instrum. Meth. A **320**, 66 (1992). T. S. Hill, Nucl. Instrum. Meth. A **418**, 32 (1998).
[8] R. Brun *et al.*, GEANT manual, CERN Program Library Long Writeup W5013, Copyright CERN, Geneva, 1993.
[9] S. Kopp *et al.* (CLEO Collaboration), Phys. Rev. D **63**, 092001 (2001).
[10] S. M. Flatte, Phys. Lett. B **63**, 224 (1976).
[11] The coupling constants $g^2_{a_0\eta\pi^0}$ and $g^2_{a_0K^+K^-}$ were re-calculated from D. V. Bugg, V. V. Anisovich, A. Sarantsev, B. S. Zou, Phys. Rev. D **50**, 4412 (1994).
[12] E. M. Aitala *et al.* (E791 Collaboration), Phys. Rev. Lett. **89**, 121801 (2002).
[13] K. Kinoshita *et al.* (CLEO Collaboration), Phys. Rev. D **43**, 2836 (1991).
[14] M. Procario *et al.* (CLEO Collaboration), Phys. Rev. D **48**, 4007 (1993).